Article

Immunity

The Inhibitory Receptor NKG2A Sustains Virus-Specific CD8+ T Cells in Response to a Lethal Poxvirus Infection

Graphical Abstract

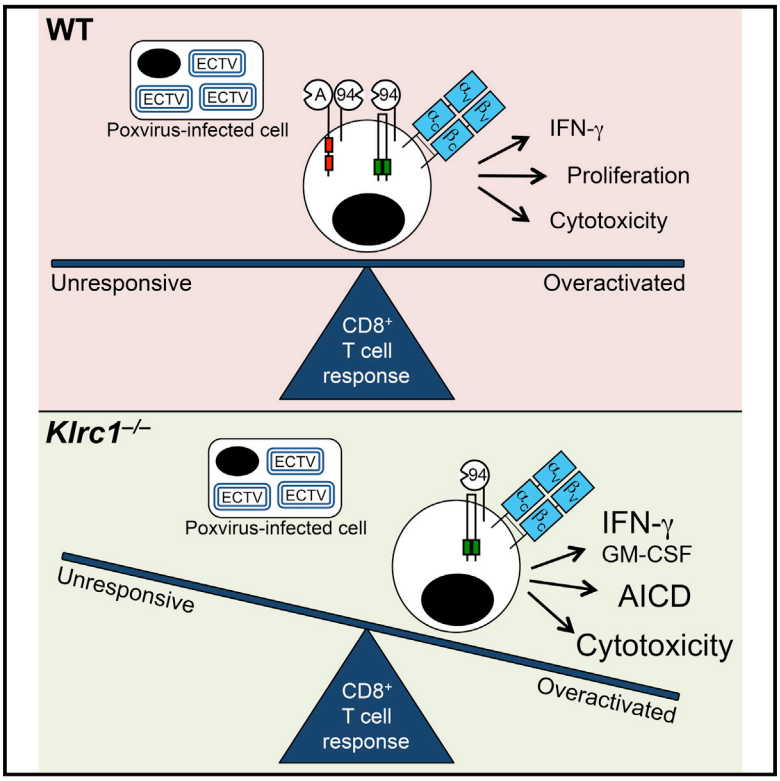

Highlights

- Control of lethal poxvirus infection requires NKG2A
- NKG2A limits excessive activation and apoptosis within virus-specific CD8+ T cells
- NKG2C and NKG2E are not expressed on the surface of mouse NK cells and CD8+ T cells
- Qa-1 is preferentially expressed on B cells in ECTV-infected tissues

Authors

Aaron S. Rapaport, Jill Schriewer, Susan Gilfillan, ..., Wayne M. Yokoyama, R. Mark L. Buller, Marco Colonna

Correspondence

mcolonna@pathology.wustl.edu

In Brief

NK cells and T cells express a variety of inhibitory receptors that differentially regulate cell survival and effector functions. Here, Colonna and colleagues demonstrate that NKG2A limits excessive activation and apoptosis of CD8+ T cells in vivo and that this function is required to resist infection with ectromelia virus.

Accession Numbers

GSE74780

Rapaport et al., 2015, Immunity *43*, 1112–1124
December 15, 2015 ©2015 Elsevier Inc.
http://dx.doi.org/10.1016/j.immuni.2015.11.005

CellPress

Immunity
Article

The Inhibitory Receptor NKG2A Sustains Virus-Specific CD8$^+$ T Cells in Response to a Lethal Poxvirus Infection

Aaron S. Rapaport,[1] Jill Schriewer,[2] Susan Gilfillan,[1] Ed Hembrador,[2] Ryan Crump,[2] Beatrice F. Plougastel,[3] Yaming Wang,[1] Gaelle Le Friec,[1,6] Jian Gao,[3] Marina Cella,[1] Hanspeter Pircher,[4] Wayne M. Yokoyama,[3,5] R. Mark L. Buller,[2] and Marco Colonna[1,*]

[1]Department of Pathology and Immunology, Washington University School of Medicine, 660 S. Euclid, St. Louis, MO 63110, USA
[2]Department of Molecular Microbiology and Immunology, Saint Louis University Health Sciences Center, 1402 South Grand Blvd, St. Louis, MO 63104, USA
[3]Rheumatology Division, Department of Medicine, Washington University School of Medicine, 660 S. Euclid, St. Louis, MO 63110, USA
[4]Institute of Immunology, Center for Microbiology and Hygiene, University Medical Center Freiburg, Hermann-Herder Strasse 11, 79104 Freiburg, Germany
[5]Howard Hughes Medical Institute, Washington University School of Medicine, 660 S. Euclid, St. Louis, MO 63110, USA
[6]Present address: Division of Transplant Immunology and Mucosal Biology, MRC Centre for Transplantation, King's College London, Guy's Hospital, Great Maze Pond, London SE1 9RT, UK
*Correspondence: mcolonna@pathology.wustl.edu
http://dx.doi.org/10.1016/j.immuni.2015.11.005

SUMMARY

CD8$^+$ T cells and NK cells protect from viral infections by killing virally infected cells and secreting interferon-γ. Several inhibitory receptors limit the magnitude and duration of these anti-viral responses. NKG2A, which is encoded by *Klrc1*, is a lectin-like inhibitory receptor that is expressed as a heterodimer with CD94 on NK cells and activated CD8$^+$ T cells. Previous studies on the impact of CD94/NKG2A heterodimers on anti-viral responses have yielded contrasting results and the in vivo function of NKG2A remains unclear. Here, we generated *Klrc1*$^{-/-}$ mice and found that NKG2A is selectively required for resistance to ectromelia virus (ECTV). NKG2A functions intrinsically within ECTV-specific CD8$^+$ T cells to limit excessive activation, prevent apoptosis, and preserve the specific CD8$^+$ T cell response. Thus, although inhibitory receptors often cause T cell exhaustion and viral spreading during chronic viral infections, NKG2A optimizes CD8$^+$ T cell responses during an acute poxvirus infection.

INTRODUCTION

CD8$^+$ T cells and NK cells contribute to host defense against viral infections by killing virally infected cells and secreting interferon-γ (IFN-γ) (Biron, 2010). Both CD8$^+$ T cells and NK cells are equipped with multiple inhibitory receptors that control the magnitude and duration of cytotoxic lymphocyte responses (Odorizzi and Wherry, 2012). These receptors can instigate disparate impacts on anti-viral responses. When cognate ligands are expressed on infected cells, inhibitory receptors control the release of lytic mediators and IFN-γ. This process might reduce tissue damage and immunopathology during acute infections (Frebel et al., 2012; Rygiel et al., 2009) but can facilitate T cell exhaustion and viral replication during chronic viral infections (Odorizzi and Wherry, 2012). Some viruses encode ligands that engage NK cell and CD8$^+$ T cell inhibitory receptors to impede killing of virally infected cells and facilitate viral replication (Lanier, 2008). When cognate ligands are expressed on dendritic cells (DCs) or T cells, inhibitory receptors might prevent NK-cell-mediated lysis of DCs or T cells that participate in the adaptive immune response (Lu et al., 2007; Waggoner et al., 2010, 2012; Xu et al., 2014). In this case, inhibitory receptors might accelerate the clearance of virally infected cells but also promote excessive adaptive responses, causing tissue damage and immunopathology.

NKG2A is an inhibitory receptor expressed on a subset of NK cells and activated CD8$^+$ T cells. It belongs to a family of lectin-like cell receptors that comprise three distinct isoforms, NKG2A (encoded by *Klrc1*), NKG2C (encoded by *Klrc2*), and NKG2E (encoded by *Klrc3*), collectively called NKG2X. NKG2A pairs with CD94 (encoded by *Klrd1*) to form a heterodimer that binds the non-classical class I molecule Qa-1 in mice (Vance et al., 1998; Zeng et al., 2012) and human leukocyte antigen E (HLA-E) in humans (Braud et al., 1998; Lee et al., 1998; Sullivan et al., 2007). The dominant peptide bound to Qa-1, named Qdm, is derived from the leader sequences of mouse major histocompatibility complex (MHC) class I molecules H-2D and H-2L (Aldrich et al., 1994; Zeng et al., 2012). NKG2A transmits intracellular inhibitory signals by recruiting the protein tyrosine phosphatases SHP1 and SHP2 (Kabat et al., 2002; Le Dréan et al., 1998). NKG2C and NKG2E also pair with CD94 to bind Qa-1 (Vance et al., 1999). However, NKG2C and NKG2E transmit activating signals through the transmembrane adaptor DAP12, which recruits the protein tyrosine kinases Syk and ZAP70 (Taylor et al., 2000). Whereas NKG2C and NKG2E directly bind DAP12 through a salt bridge in their transmembrane domains in humans (Call et al., 2010), NKG2C and NKG2E associate with DAP12 indirectly in mice, because murine CD94 forms a salt bridge with DAP12 in its transmembrane region (Saether et al., 2011).

Previous investigations of CD94/NKG2A heterodimer function during viral infections using blocking antibodies or Qa-1-deficient mice have yielded contrasting results. CD94/NKG2A heterodimers inhibited $CD8^+$ T cell cytotoxic responses to polyoma virus (Moser et al., 2002) and inhibited NK-cell-mediated killing of cells infected with human cytomegalovirus (HCMV) (Tomasec et al., 2000). In contrast, CD94/NKG2A heterodimers did not inhibit $CD8^+$ T cell effector functions during lymphocytic choriomeningitis virus (LCMV) or *Listeria monocytogenes* (Lm) infections (McMahon et al., 2002; Miller et al., 2002). Another report suggested that CD94/NKG2X complexes might protect both NK and T cells from apoptosis during Lm infection (Gunturi et al., 2003). More recently, it was shown that CD94-deficient (*Klrd1*$^{-/-}$) mice are highly susceptible to mouse orthopoxvirus ectromelia virus (ECTV) infection (Fang et al., 2011). However, susceptibility to infection was not attributed to lack of CD94/NKG2A heterodimers, but rather to loss of the activating CD94/NKG2E/DAP12 complex, which possibly triggered lysis of ECTV-infected cells through recognition of a viral peptide bound to Qa-1. Finally, *Klrc1*$^{-/-}$ mice had more immunopathology during influenza and adenovirus infections (Ely et al., 2014).

To unequivocally determine the function of NKG2A during viral infections in vivo, we generated *Klrc1*$^{-/-}$ mice on the C56BL/6 background and tested immune responses against LCMV, VSV, vaccinia virus (VV), and ECTV. We found that *Klrc1*$^{-/-}$ mice are uniquely susceptible to infection by ECTV and that NKG2A is required to sustain virus-specific $CD8^+$ T cells by preventing activation-induced cell death (AICD).

RESULTS

Mouse NK Cells Lack Surface Expression of NKG2C and NKG2E

To generate *Klrc1*$^{-/-}$ mice, we targeted exons 1 through 4 of *Klrc1* (Figure S1A). We confirmed that mouse splenocytes lack *Klrc1* transcripts but maintain transcription of *Klrc2* and *Klrc3* (Figure S1B), indicating that the deletion is limited to *Klrc1*. NK, NKT, and T cells from spleens, livers, and lungs were present at similar frequencies in *Klrc1*$^{-/-}$ and WT control mice (Figure S1C). NK cells from *Klrc1*$^{-/-}$ mice were mature, as judged by CD11b and CD27 expression. Thus, NKG2A plays no obvious role in the development of NK or T cells. Splenic NK cells also expressed normal amounts of KLRG1, CD49b, Ly49 family members, and NKG2D (Figure S1D), indicating that the receptor repertoire is undisturbed by the NKG2A deletion. These results are consistent with previous studies on DBA/2J mice, which are naturally deficient for CD94, yet exhibit no developmental defects (Vance et al., 2002).

To verify that NKG2A expression was completely ablated in *Klrc1*$^{-/-}$ mice, we assessed cell surface expression by flow cytometry with an antibody that recognizes all three mouse NKG2X family members. Approximately 40% of WT splenic NK cells expressed NKG2X on the surface under steady-state conditions. Notably, NK cells from *Klrc1*$^{-/-}$ spleens completely lacked NKG2X surface expression (Figure 1A), suggesting that NKG2A is the only NKG2X family member expressed on the surface of mouse NK cells. Because NKG2E has been implicated in the control of ECTV (Fang et al., 2011), we monitored NKG2X expression on NK cells after ECTV infection. However, NK cells from *Klrc1*$^{-/-}$ spleens completely lacked NKG2X surface expression even after infection. We next assessed NKG2X expression on T cells. Only a small population of naive WT $CD8^+$ T cells was positive for NKG2X expression. $CD8^+$ T cells from *Klrc1*$^{-/-}$ spleens also expressed little to no NKG2X under homeostatic conditions. After infection with ECTV, approximately one-quarter of WT $CD8^+$ T cells were $NKG2X^+$, whereas only 0.4% of *Klrc1*$^{-/-}$ $CD8^+$ T cells were $NKG2X^+$ (Figure 1B). We corroborated these observations by staining NK cells and activated $CD8^+$ T cells with both anti-NKG2ACE and an antibody specific for $NKG2A^{B6}$. Both antibodies stained each WT population equivalently and did not mark any cells from *Klrc1*$^{-/-}$ samples (Figure S1E). These data are in agreement with previous studies showing that NKG2A comprises almost all of the NKG2X molecules found on mouse NK cells and activated $CD8^+$ T cells (Kawamura et al., 2009; Vance et al., 2002).

CD94 Is Surface Expressed with DAP12 in the Absence of NKG2X

Analysis of CD94 expression confirmed lack of detectable NKG2C or NKG2E associated with CD94. WT NK cells from uninfected and ECTV-infected mice showed two peaks of CD94 expression; the higher peak corresponded to CD94/NKG2X complexes, whereas the lower peak lacked NKG2X (Figure 1C, top, and 1A). The $CD94^{hi}$ peak was undetectable on *Klrc1*$^{-/-}$ NK cells, indicating that NK cells express CD94/NKG2X complexes exclusively in the form of CD94/NKG2A heterodimers. $CD8^+$ T cells in both WT and *Klrc1*$^{-/-}$ mice expressed similar amounts of CD94 after ECTV infection. However, *Klrc1*$^{-/-}$ $CD8^+$ T cells expressed CD94 overwhelmingly without NKG2X proteins (Figure 1C, bottom, and 1B). Our CD94 expression analysis therefore demonstrates that although mouse CD94 preferentially associates with NKG2A, it is expressed in lower amounts ($CD94^{lo}$) in the absence of NKG2A. Coupled with the lack of NKG2C and NKG2E expression in the mouse, this indicates that CD94 might also function as part of a yet-to-be-characterized receptor complex.

A recent study has shown that mouse CD94 contains a charged transmembrane residue capable of associating directly with the adaptors DAP10 and DAP12 (Saether et al., 2011). We therefore sought to test whether $CD94^{lo}NKG2X^-$ NK cells required DAP10 (encoded by *Hcst*) or DAP12 (encoded by *Tyrobp*) for surface expression of CD94. We found that the $CD94^{lo}$ population was markedly reduced in *Tyrobp*$^{-/-}$ NK cells, whereas it was maintained in *Hcst*$^{-/-}$ NK cells (Figure 1D). For controls, we confirmed that Ly49H expression was largely ablated in *Tyrobp*$^{-/-}$ NK cells and that NKG2X expression was maintained (Figure 1E). This indicates that in mouse NK cells, CD94 itself might function as a DAP12-associated activating NK receptor. Because activated $CD8^+$ T cells express DAP10 but not DAP12, we also asked whether CD94/NKG2A heterodimers require DAP10 for surface expression. As expected, we found that expression of this heterodimer was maintained on *Hcst*$^{-/-}$ nonspecific and antigen-specific $CD8^+$ T cells (Figure 1F). It is likely that in the absence of NKG2A, CD94 surface expression requires DAP10, although a formal demonstration requires the generation of *Klrc1*$^{-/-}$ × *Hcst*$^{-/-}$ mice. Taken together, these data indicate that two CD94 complexes are found on the surface

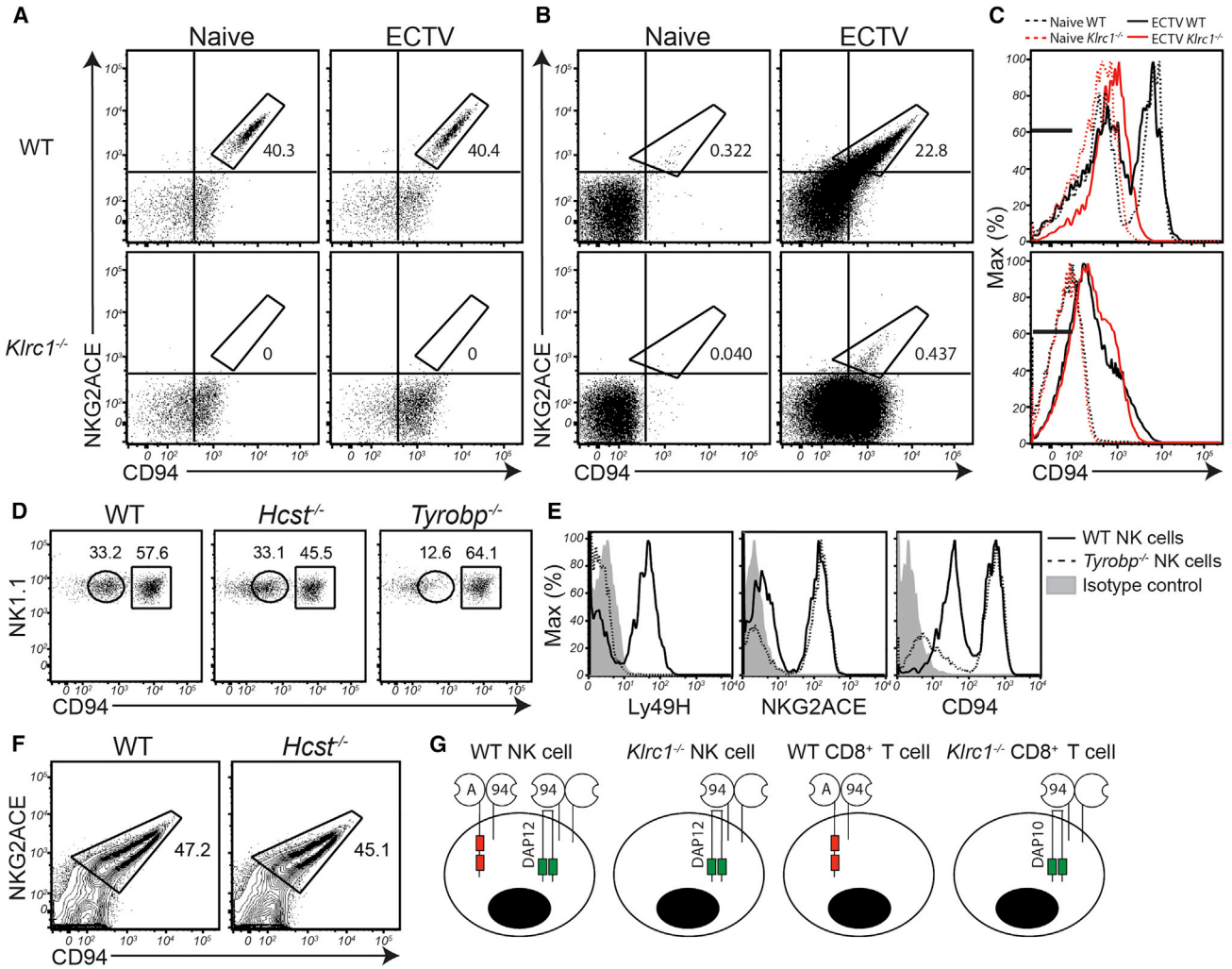

Figure 1. NK and CD8$^+$ T Cells Do Not Express NKG2C or NKG2E on the Cell Surface

(A and B) Spleens were analyzed by flow cytometry for surface expression of NKG2ACE and CD94 under naive conditions or 7 dpi of f.p. with 1,000 PFU ECTV-Moscow. NK cells (A) and CD8$^+$ T cells (B) are depicted.

(C) CD94 expression was measured on splenic NK cells (top) and CD8$^+$ T cells (bottom). Both histograms depict naive WT cells (black dashed line), naive *Klrc1*$^{-/-}$ cells (red dashed line), ECTV-stimulated WT cells (black solid line), ECTV-stimulated *Klrc1*$^{-/-}$ cells (red solid line). Cells stained with isotype control antibodies fell within black bars.

(D) Naive splenic NK cells from WT, *Hcst*$^{-/-}$, and *Tyrobp*$^{-/-}$ mice were assessed for CD94^{lo} and CD94^{hi} populations.

(E) Ly49H, NKG2ACE, and CD94 expression was assessed on WT and *Tyrobp*$^{-/-}$ naive splenic NK cells.

(F) NKG2ACE and CD94 expression was measured on total CD8$^+$ T cells from WT and *Hcst*$^{-/-}$ mice. Mice were infected with LCMV clone 13 and on day 8 p.i., spleens were isolated.

(G) Schematic of NKG2A and CD94 surface expression on mouse killer cells. Data are representative of at least three independent experiments.

Further supporting evidence can be found in Figure S1 and Table S1.

of mouse killer cells: one containing NKG2A and another that lacks a *Klrc*-encoded partner (Figure 1G).

NKG2A Is Important for the Control of ECTV Infection

Because a previous study indicated that an intact CD94-dependent NK cell response is required to resist infection to ECTV (Fang et al., 2011) and we were unable to detect expression of either NKG2C or NKG2E on NK cells, we hypothesized that NKG2A might play an important role in controlling this infection. Therefore, we challenged *Klrc1*$^{-/-}$ mice with a standard 1,000 PFU dose of ECTV in the footpad and observed that *Klrc1*$^{-/-}$ male mice were very susceptible to this infection, evident by increased morbidity and mortality (Figures 2A and 2B) as well as elevated viremia and splenic viral loads 6–10 days after infection (Figure 2C). *Klrc1*$^{-/-}$ female mice also had higher viremia and splenic viral loads than did WT female mice, although morbidity and mortality were similar. It has been shown that males are more vulnerable than females in mouse strains susceptible to ECTV (Brownstein and Gras, 1995). Here, we also noted that males, in general, had higher viremia and liver titers than their female counterparts (Figure 2C). Thus, the severe susceptibility of the *Klrc1*$^{-/-}$ males appears to be a combination of a general male

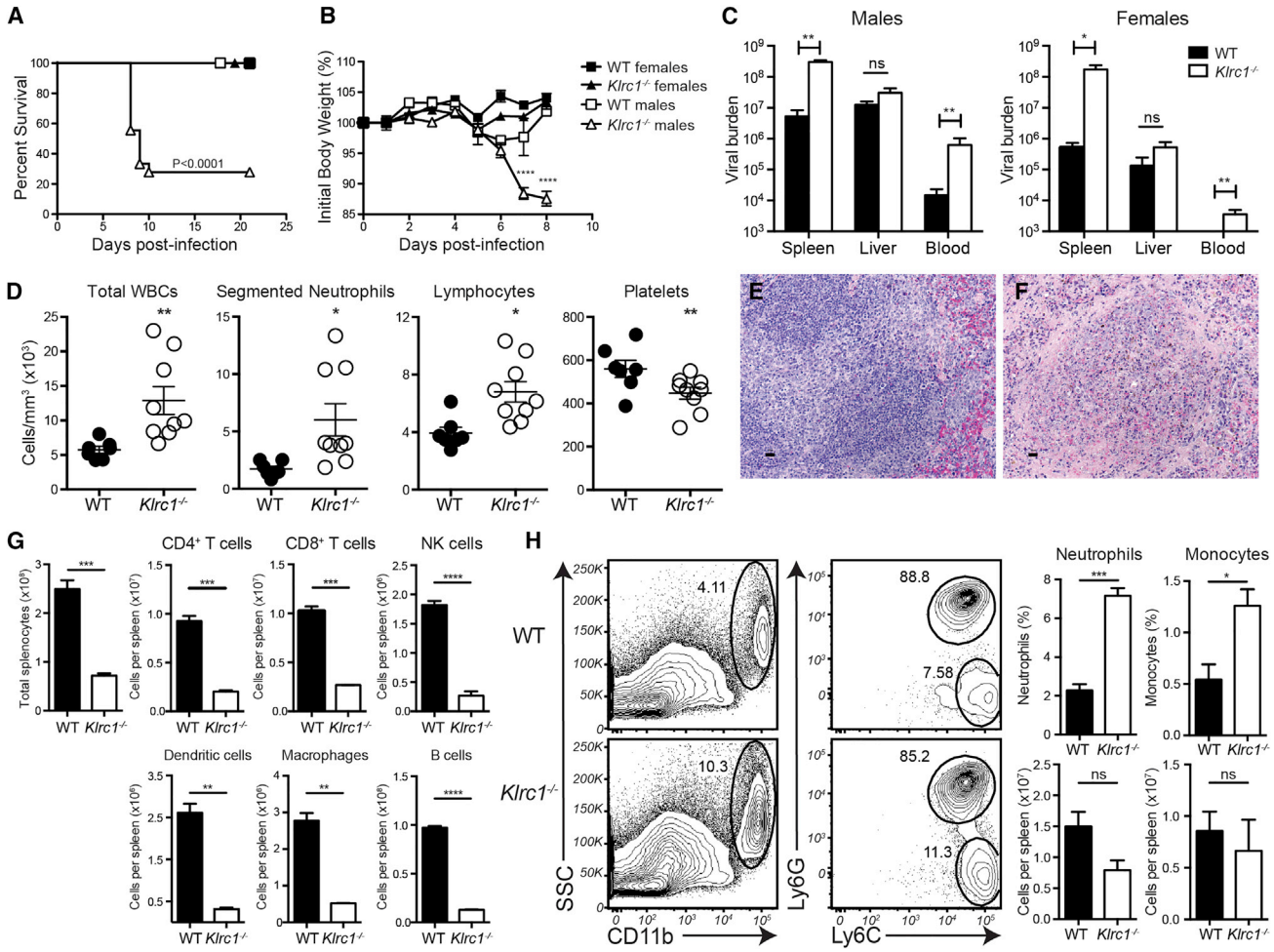

Figure 2. *Klrc1*$^{-/-}$ Mice Are More Susceptible to ECTV Infection

(A and B) WT and *Klrc1*$^{-/-}$ mice were infected with ECTV and monitored for survival (A) and body weight (B) over time.

(C) Viral load was assessed at 6 dpi. ECTV genome load in the blood was measured by quantitative RT-PCR. Spleen and liver viral loads were determined by plaque assay. Black bars indicate WT tissues and white bars indicate *Klrc1*$^{-/-}$ tissues.

(D) WT (black circles) and *Klrc1*$^{-/-}$ (white circles) blood was collected from ECTV-infected animals 6 dpi and was assessed by complete white blood cell (WBC) counts and WBC differentials (segmented neutrophil, lymphocyte, and platelet counts).

(E and F) WT (E) and *Klrc1*$^{-/-}$ (F) spleens were fixed and stained with H&E 6 dpi. Original magnification 40×. Scale bars represent 20 μm.

(G) Total splenocyte and splenic leukocyte cell numbers were assessed 7 dpi.

(H) Neutrophil (CD11b^{+}Ly6C^{+}Ly6G^{+}) and monocyte (CD11b^{+}Ly6C^{+}Ly6G^{-}) frequencies and cell numbers were assessed 7 dpi.

Images in (E) and (F) are representative of two independent experiments. All other data were pooled from at least two independent experiments and were analyzed by multiple t tests. Mean ± SEM is represented on relevant graphs. Further supporting evidence can be found in Figure S2 and Table S1.

vulnerability to ECTV coupled with a bona fide role for NKG2A in the anti-ECTV response.

We next assessed the blood for any disruptions in cellularity. At 7 days after infection, we noted significant increases in total white blood cell (WBC) counts, specifically in the number of neutrophils and lymphocytes, concomitant with a corresponding reduction in the number of platelets per volume of blood in *Klrc1*$^{-/-}$ mice (Figure 2D). Marked histopathology was also evident in hematoxylin and eosin (H&E) staining of spleen sections from *Klrc1*$^{-/-}$ mice, which were highly acellular with disrupted tissue architecture compared to WT controls 7 days after infection (Figures 2E and 2F). The acellularity of *Klrc1*$^{-/-}$ spleens was attributable to reduction in multiple leukocyte populations, including NK cells, T cells, B cells, dendritic cells, and macrophages (Figure 2G). Neutrophil and monocyte frequencies, however, were relatively increased and numbers were largely maintained in *Klrc1*$^{-/-}$ spleens, indicating that any perturbation due to the anti-viral response also resulted in accrual of neutrophils and monocytes (Figure 2H). In contrast, livers, lungs, and kidneys from *Klrc1*$^{-/-}$ mice appeared to remain largely intact and comparable to WT tissues after ECTV infection (data not shown). Therefore, ECTV infection causes pathology preferentially in the spleen and blood of *Klrc1*$^{-/-}$ mice.

Klrc1$^{-/-}$ Mice Harbor an Otherwise Intact *Klrc* Locus and Susceptibility to ECTV Segregates with the Targeted Mutation of *Klrc1*

We wanted to ensure that these results were wholly attributable to elimination of NKG2A expression and not to more drastic

disruption of the *Klrc* locus, possibly engendered during targeting. Therefore we sequenced the entire *Klrc* locus to confirm that it remained intact (apart from the targeted deletion of *Klrc1*) in the *Klrc1*$^{-/-}$ mice. The only mutations found within the *Klrc1*$^{-/-}$ line were an approximately 2.5 kb deletion corresponding to the targeted deletion of *Klrc1* and few surrounding point mutations that were probably introduced during PCR amplification of the homology arms of the targeting construct (Table S1). Furthermore, as mentioned previously, *Klrc2* and *Klrc3* transcripts were present at similar levels in the spleens of both WT and *Klrc1*$^{-/-}$ mice (Figure S1B), indicating that the deletion and point mutations did not disrupt transcriptional regulation of the *Klrc* locus. Also, as noted in Figure 1, CD94 expression was equivalent to WT in the *Klrc1*$^{-/-}$ line. Because *Klrc2*, *Klrc3*, and *Klrd1* are the genes nearest to the targeted region, their unaltered expression indicates that the targeted deletion of *Klrc1* is specific and that the *Klrc1*$^{-/-}$ strain contains an otherwise intact *Klrc* locus.

To rule out the possibility that the targeted ES clone used to generate the mice contained other chromosomal mutations, particularly on the Y chromosome, that might be responsible for the ECTV phenotype, we bred male and female *Klrc1*$^{-/-}$ mice to C57BL/6 WT mice to generate heterozygotes; these were intercrossed to generate two groups of *Klrc1*$^{-/-}$, *Klrc1*$^{-/+}$, and *Klrc1*$^{+/+}$ F2 mice, one with the Y chromosome from *Klrc1*$^{-/-}$ males and the other with the Y chromosome from C57BL/6 males. The *Klrc1*$^{-/-}$ males from both groups of F2 mice were acutely susceptible to ECTV (Figures S2A–S2C), corroborating our initial observation that increased susceptibility to ECTV segregates with and is due to the targeted *Klrc1* mutation.

NKG2A Deficiency Results in Fewer ECTV-Specific CD8$^+$ T Cells that Exhibit Increased Effector Functionality

Given that mice die at 8–10 days after ECTV infection and that NK cells and CD8$^+$ T cells predominate anti-ECTV responses at this stage (Parker et al., 2007) and express NKG2A, we evaluated the impact of NKG2A deficiency on CD8$^+$ T cell and NK cell responses. The number of *Klrc1*$^{-/-}$-specific CD8$^+$ T cells was markedly reduced after ECTV infection, as judged by B8R$_{20\text{-}27}$-H2-K^b tetramer staining, indicating that NKG2A might function to enhance the accumulation of specific CD8$^+$ T cells (Figure 3A). In contrast, *Klrc1*$^{-/-}$ CD8$^+$ T cells restimulated ex vivo with the immunodominant epitope of the orthopoxvirus B8R protein (B8R$_{20\text{-}27}$) had more intracellular IFN-γ than did WT cells and expressed more CD107a, a marker of degranulation (Figure 3B). This indicates that, on a per cell basis, NKG2A inhibits effector functions of virus-specific CD8$^+$ T cells. In agreement, *Klrc1*$^{-/-}$ CD8$^+$ T cells secreted greater quantities of IFN-γ when stimulated with B8R$_{20\text{-}27}$ (Figure 3C). We also detected significantly higher quantities of IFN-γ in the sera of *Klrc1*$^{-/-}$ males at 7 dpi (Figure 3D). These data indicate that NKG2A might function to both limit CD8$^+$ T cell activation and sustain the specific CD8$^+$ T cell population in the context of ECTV infection.

Given the increased quantities of IFN-γ found in *Klrc1*$^{-/-}$ mice, we next asked whether NKG2A deficiency resulted in greater production of other cytokines by CD8$^+$ T cells. Notably, we found that more granulocyte-monocyte colony stimulating factor (GM-CSF), but not tumor necrosis factor (TNF) or interleukin-2 (IL-2), was produced by virus-specific *Klrc1*$^{-/-}$ CD8$^+$ T cells—the same T cells that produced high amounts of IFN-γ (Figures 3E–3G). GM-CSF promotes myeloid cell accrual, so these data suggest that during ECTV infection, NKG2A deficiency results specifically in polyfunctional IFN-γ^{hi}GM-CSF$^+$CD8$^+$ T cells that could contribute to the neutrophil and monocyte accumulation seen in *Klrc1*$^{-/-}$ spleens. Moreover, *Klrc1*$^{-/-}$ CD8$^+$ T cells were generally larger and more granular than their WT counterparts at 7 dpi, but did not exhibit altered skewing toward a short-lived effector cell (SLEC) population or memory precursor effector cell (MPEC) (Figures 3H and 3I), suggesting that NKG2A limits general activation of ECTV-specific CD8$^+$ T cells.

Klrc1$^{-/-}$ NK Cells Remain Functionally Intact after ECTV Infection

We assessed NK cell function in the spleen at 5.5 dpi, when NKG2A expression on CD8$^+$ T cell control appears to be important for viral control. WT and *Klrc1*$^{-/-}$ NK cells restimulated in vitro with tumor target cells expressed equivalent levels of both IFN-γ and CD107a, indicating that NK cell function is largely maintained in the absence of NKG2A (Figure 3J). To determine whether *Klrc1*$^{-/-}$ NK cell function was altered at earlier time points, when CD8$^+$ T cells were not yet primed, we quantified the viral burden in draining popliteal lymph nodes 3 days after footpad infection with ECTV (Figure 3K). We chose this time point because early resistance to ECTV is more dependent on NK cells and popliteal lymph nodes are the primary location for viral replication prior to systemic infection (Parker et al., 2007). However, there was no difference in viral burden in the popliteal lymph nodes at this time, suggesting that NKG2A plays an insignificant role in early NK cell-mediated control of ECTV infection. Thus, NKG2A expression on NK cells has no effect on the control of ECTV infection.

Klrc1$^{-/-}$ Thymocytes Develop Normally and NKG2A Marks a Population of Thymic NKT Cells

Given that NKG2A deficiency resulted in a reduced number of antiviral CD8$^+$ T cells, we sought to further assess the role of NKG2A in T cell development by analyzing thymuses of WT and *Klrc1*$^{-/-}$ mice. However, we found no differences in any thymocyte subset in *Klrc1*$^{-/-}$ mice (Figure S3A). We did observe that subsets of both CD4$^-$CD8$^-$ and CD4 single-positive cells express NKG2A (Figure S3B). We found that these cells were thymic NKT cells, as judged by co-expression of NK1.1 and CD3 and the fact that NKG2A deficiency did not alter the accumulation of these cells in the thymus (Figure S3C). Together, these data show that NKG2A is not expressed on thymocytes and does not alter thymocyte development, but does mark a population of thymic NKT cells.

Klrc1$^{-/-}$ ECTV-Specific CD8$^+$ T Cells Express Genes Associated with Lymphocyte Activation and Apoptosis

Given that NKG2A deficiency leads to excessive effector functions of CD8$^+$ T cells after ECTV infection, we sought to analyze whether NKG2A signaling altered specific transcriptional pathways associated with T cell activation. To test this, we sorted both naive and ECTV-specific CD8$^+$ T cells and analyzed the transcriptomes via microarray analysis. WT and *Klrc1*$^{-/-}$ CD8$^+$ T cell transcriptomes were broadly similar when assessed by principal component analysis (PCA) (Figure 4A). There were

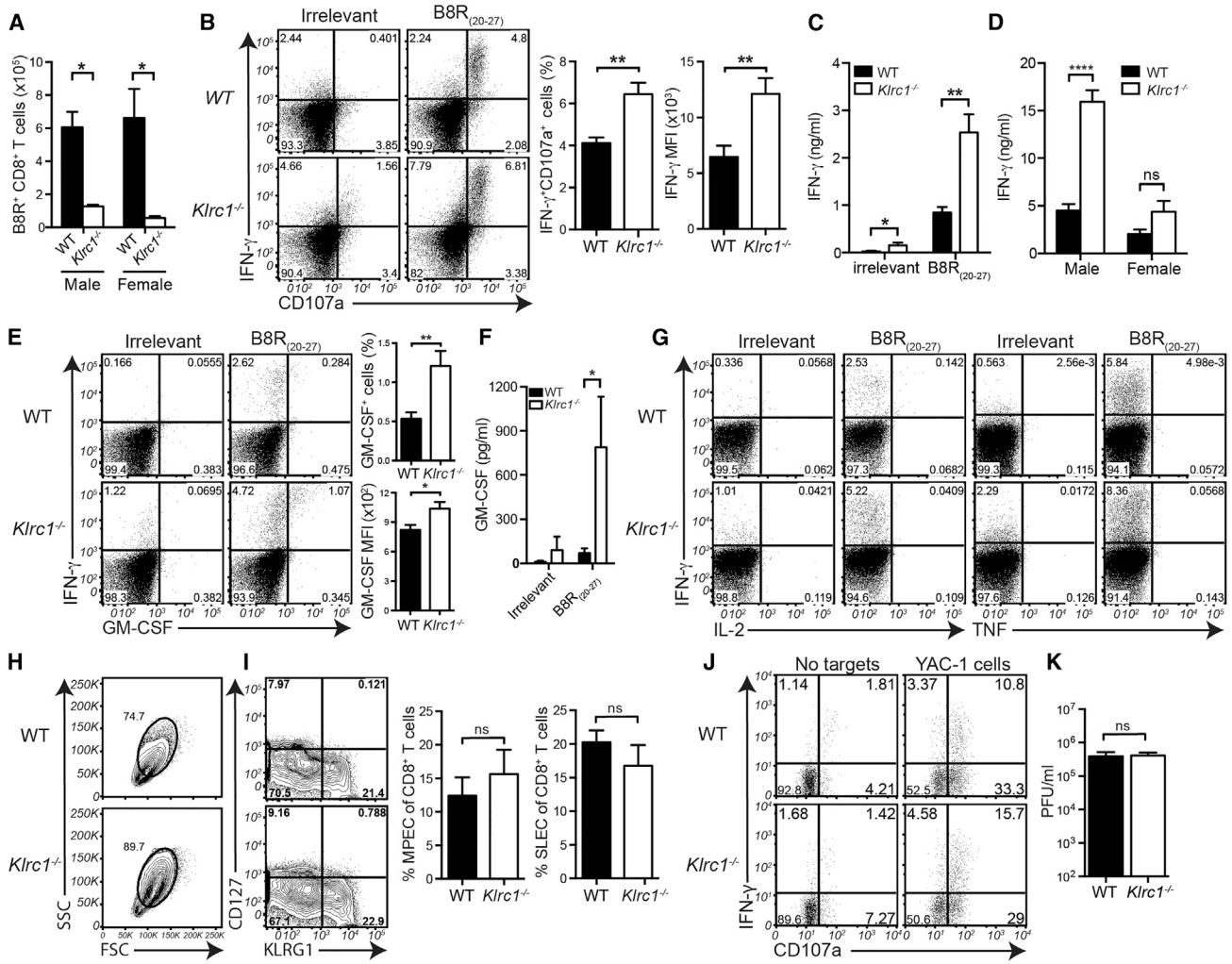

Figure 3. Characterization of WT and *Klrc1*$^{-/-}$ CD8$^+$ T Cell and NK Cell Responses to ECTV

Mice were infected with ECTV and spleens analyzed for CD8$^+$ T cell responses 7 dpi.

(A) CD3$^+$CD8$^+$B8R-H2-K^{b+} T cell numbers were quantified in spleens.

(B) WT or *Klrc1*$^{-/-}$ splenocytes were pulsed ex vivo with irrelevant SIINFEKL peptide or poxvirus-specific B8R$_{20-27}$, then assessed for CD107a and IFN-γ expression by intracellular staining of CD3$^+$CD8$^+$ lymphocytes. The frequency of CD107a$^+$IFN-γ$^+$CD8$^+$ T cells and MFI of IFN-γ$^+$ cells were quantified in WT (black bars) and *Klrc1*$^{-/-}$ (white bars) splenocytes.

(C) Splenocytes were incubated overnight with irrelevant or B8R$_{20-27}$ peptides to restimulate CD8$^+$ T cells. IFN-γ accumulation in the supernatant was quantified by bead array.

(D) IFN-γ concentration was measured from the sera of ECTV-infected mice by bead array.

(E) Splenocytes were treated as in (A), then assessed for GM-CSF intracellular content. GM-CSF$^+$ cell frequency and MFI of GM-CSF$^+$ cells are shown.

(F) Splenocytes were treated as in (C). GM-CSF accumulation in the supernatant was quantified by ELISA.

(G) Splenocytes were treated as in (A), and TNF or IL-2 intracellular content was determined.

(H) CD3$^+$CD8$^+$ lymphocyte blasting was assessed by FSC and SSC.

(I) Total CD3$^+$CD8$^+$ lymphocytes were analyzed for KLRG1 and CD127 expression. Frequency of SLEC (KLRG1$^+$CD127$^-$) and MPEC (KLRG1$^-$CD127$^+$) populations are shown.

(J) Expression of IFN-γ and CD107a in splenic NK cells were measured 5.5 dpi. Splenocytes were incubated with or without 1 × 10^5 YAC-1 targets cells, then stained for NK cell markers and intracellular IFN-γ. Dot plots show CD107a and IFN-γ expression on CD3$^-$NK1.1$^+$ NK cells.

(K) Viral load in popliteal lymph nodes was assessed by plaque assay 3 dpi.

All data are pooled from at least two independent experiments and were analyzed by multiple t tests. Mean ± SEM is represented on relevant graphs. Further supporting evidence can be found in Figure S3.

only mild variations in individual gene expression profiles of naive CD8$^+$ T cells (Figure 4B). However, there were wider variations in the expression of 225 transcripts by ECTV-specific WT and *Klrc1*$^{-/-}$ CD8$^+$ T cells (Figures 4C and 4D), which associated with specific pathways as judged by gene ontology pathway analysis (Figure 4E). *Klrc1*$^{-/-}$ cells contained an overabundance of transcripts falling within five categories of stimulatory pathways, including responses to stress and stimuli, cell proliferation,

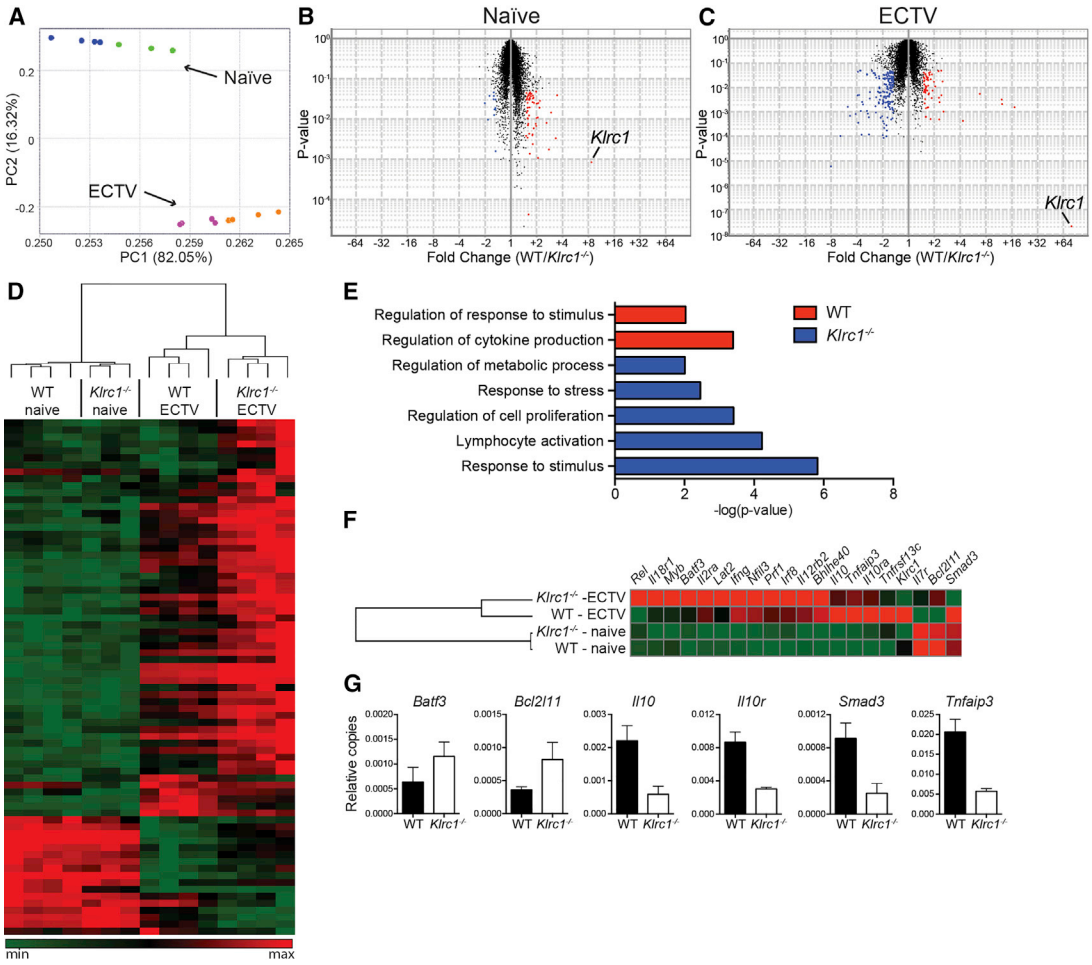

Figure 4. Differential Expression of Genes Associated with Lymphocyte Activation in *Klrc1*$^{-/-}$ ECTV-Specific CD8$^+$ T Cells

CD3$^+$CD8$^+$B8R-H2-K^{b+} T cells were sorted from WT and *Klrc1*$^{-/-}$ mice infected with ECTV and total RNA was isolated. As a control, RNA was isolated from total CD3$^+$CD8$^+$ T cells of naive WT and *Klrc1*$^{-/-}$ mice. Transcriptomes of all RNA samples were assessed by microarray analysis.

(A) Principal component analysis of total naive and ECTV-specific CD8$^+$ T cells. Naive WT (blue dots), naive *Klrc1*$^{-/-}$ (green dots), WT infected (purple dots), and *Klrc1*$^{-/-}$ infected (orange dots) samples are shown.

(B and C) Volcano plots of naive WT versus naive *Klrc1*$^{-/-}$ CD8$^+$ T cells (B) or ECTV-specific WT versus ECTV-specific *Klrc1*$^{-/-}$ CD8$^+$ T cells (C). Transcripts differentially expressed in *Klrc1*$^{-/-}$ cells (blue dots) versus WT cells (red dots) are labeled. *Klrc1* is also indicated in both plots.

(D) Heatmap of all genes differentially expressed between WT and *Klrc1*$^{-/-}$ CD8$^+$ T cells. The scale ranges from minimum (green boxes) to medium (black boxes) to maximum (red boxes) relative expression.

(E) Gene ontology pathway analysis of ECTV-specific CD8$^+$ T cells. Red bars indicate pathways overrepresented in WT cells and blue bars indicate pathways overrepresented in *Klrc1*$^{-/-}$ cells.

(F) Heatmap of genes representative of the differentially expressed pathways depicted in (E). Coloration is equivalent to that used in (D).

(G) Quantitative RT-PCR amplification of relevant genes to validate microarray analysis data. All transcripts are shown relative to *Gapdh* copy number.

Mean ± SEM is represented on relevant graphs.

and lymphocyte activation. Several individual transcripts overabundant in *Klrc1*$^{-/-}$ cells were indicative of CD8$^+$ T cell activation, including *Ifng*, *Prf1*, *Rel*, *Batf3*, and *Bhlhe40* (Figure 4F). Upregulation of *Bhlhe40* most likely explains the augmented production of GM-CSF by virus-specific *Klrc1*$^{-/-}$ CD8$^+$ T cells, because Bhlhe40 positively regulates the production of GM-CSF (Lin et al., 2014). Importantly, *Klrc1*$^{-/-}$ cells also overexpressed *Bcl2l11*, which encodes Bim, a key pro-apoptotic mediator. In contrast, WT ECTV-specific CD8$^+$ T cells featured an overabundance of transcripts that fell within immunoregulatory pathways, including *Il10*, *Il10r*, *Smad3*, and *Tnfaip3* (Figure 4F). Differential expression of relevant genes was further verified by quantitative real-time PCR analysis of ECTV-specific CD8$^+$ T cell cDNA (Figure 4G). Overall, transcriptional changes in *Klrc1*$^{-/-}$ ECTV-specific CD8$^+$ T cells indicate that these cells are more activated than their WT counterparts and are potentially more susceptible to apoptosis.

Klrc1$^{-/-}$-Specific CD8$^+$ T Cells Are Intrinsically Vulnerable to Apoptosis

Our previous data suggest that NKG2A limits effector functions of ECTV-specific CD8$^+$ T cells, while sustaining a higher number

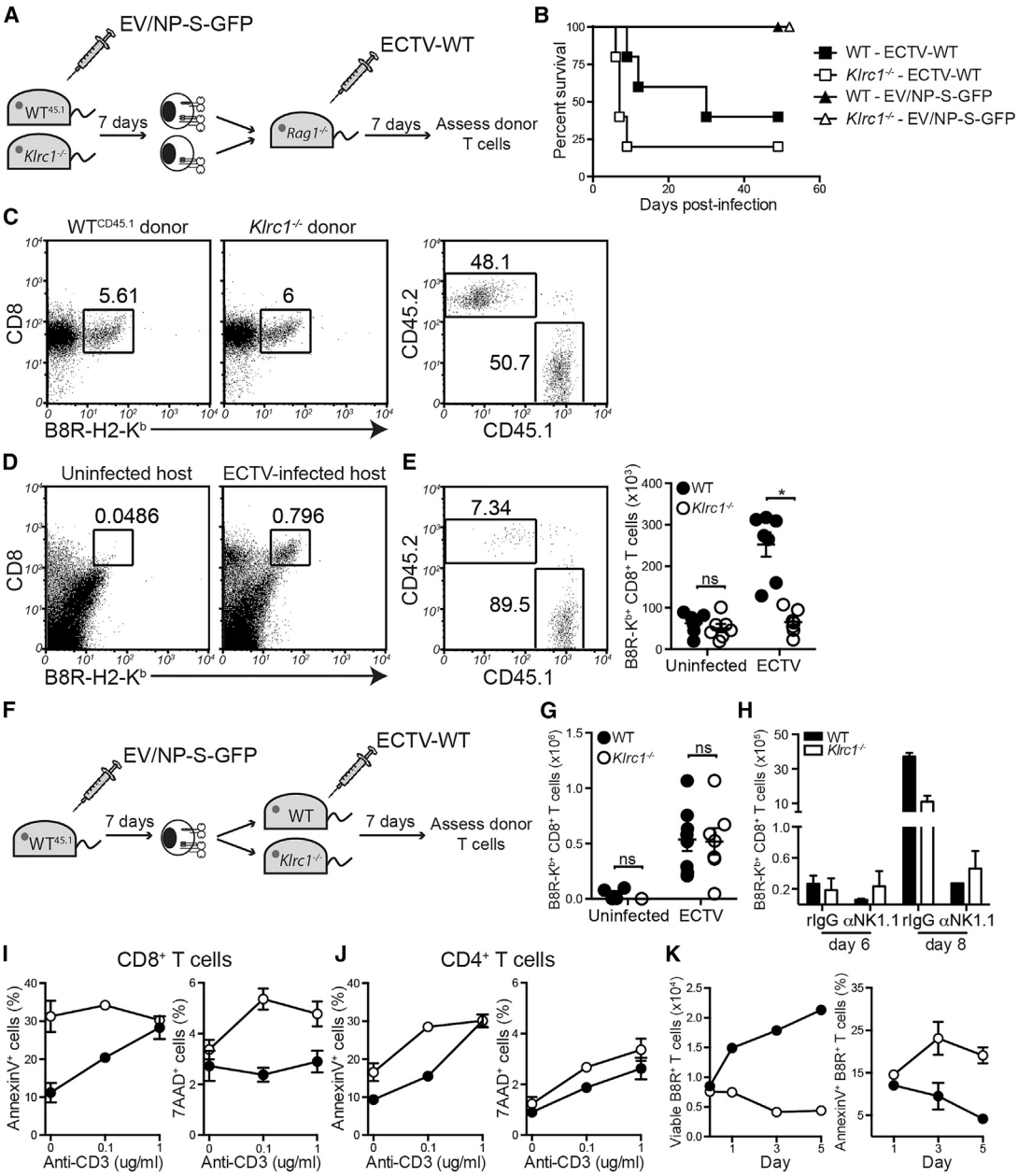

Figure 5. NKG2A Limits Apoptosis of Virus-Specific CD8⁺ T Cells in a Cell-Intrinsic Manner

(A) Schematic to test for a cell-intrinsic mechanism of NKG2A function in ECTV-specific CD8⁺ T cell survival.

(B) WT and *Klrc1*$^{-/-}$ male mice were infected f.p. with either 7,000 PFU ECTV-WT or 9,000 PFU EV/NP-S-GFP and survival was monitored for 7.5 weeks after infection.

(C) WT$^{CD45.1}$ and *Klrc1*$^{-/-}$ mice were immunized with 5,000 PFU ECTV-ova f.p. and CD8⁺ T cells were enriched from spleens 7 dpi via MACS selection. Cells were then mixed at a 1:1 ratio of B8R-H2-K^{b+} cells and adoptively transferred into *Rag1*$^{-/-}$ hosts.

(D) *Rag1*$^{-/-}$ hosts were either left uninfected or infected with ECTV-WT for 7 days, then analyzed for B8R-H2-K^{b+} CD8⁺ T cells.

(E) Frequencies of WT and *Klrc1*$^{-/-}$ CD3⁺CD8⁺B8R-H2-K^{b+} cells from *Rag1*$^{-/-}$ spleens 7 dpi with ECTV-WT. Total CD3⁺CD8⁺B8R-H2-K^{b+} cell numbers from naive or ECTV-WT-infected *Rag1*$^{-/-}$ spleens are shown on the right.

(F) Schematic to test for a cell-extrinsic mechanism of NKG2A function in ECTV-specific CD8⁺ T cells.

(G) Total number of specific donor cells (CD45.1⁺CD3⁺CD8⁺B8R-H2-K^{b+} cells) isolated from naive hosts or ECTV-WT-infected hosts.

(H) Mice were treated with either control or NK-cell-depleting antibody prior to infection with 200 PFU ECTV-WT. On days 6 or 8 post-infection, spleens were isolated and antigen-specific CD8⁺ T cell numbers were quantified.

(I) WT and *Klrc1*$^{-/-}$ splenocytes were isolated 7 days after ECTV infection and put in culture in the presence or absence of plate-bound anti-CD3 antibody. After 2 days, CD8⁺ T cells were assessed for Annexin V (left) and 7AAD (right).

(J) Cells were prepared as in (I) and CD4⁺ T cells were analyzed.

(legend continued on next page)

of specific CD8$^+$ T cells. These data, combined with the overabundance of *Bcl2l11* transcript in *Klrc1*$^{-/-}$-specific CD8$^+$ T cells, led us to hypothesize that NKG2A has two distinct functions within CD8$^+$ T cells: to limit excessive effector function and to prevent unnecessary apoptosis. To test this in vivo, we designed an adoptive transfer system that would allow us to observe *Klrc1*$^{-/-}$ B8R-specific CD8$^+$ T cells in competition with WT B8R-specific CD8$^+$ T cells during ECTV infection (Figure 5A). To generate a pool of B8R-specific T cells, CD45.1 WT mice and CD45.2 *Klrc1*$^{-/-}$ mice were infected with an ova peptide-transgenic strain of ECTV (EV/NP-S-GFP) that causes less mortality in *Klrc1*$^{-/-}$ mice (Figure 5B). Approximately 1 week after infection, splenic CD8$^+$ T cells from each strain were enriched and assessed for TCR specificity by staining with B8R-H2-K^b tetramers, and then mixed at a 1:1 ratio of tetramer$^+$ cells (Figure 5C). This mixture was injected i.v. into *Rag1*$^{-/-}$ hosts, which were infected with WT-ECTV 1 day after transfer. As a control, some *Rag1*$^{-/-}$ mice were given the T cell mixture, but not infected with virus. Uninfected *Rag1*$^{-/-}$ spleens did not harbor a significant population of specific T cells 8 days after transfer. Hosts that were infected with WT virus, however, had a noticeable population of B8R-specific CD8$^+$ T cells (Figure 5D). In the infected hosts, WT (CD45.1)-specific donor cells were more frequent and significantly outnumbered *Klrc1*$^{-/-}$ (CD45.2) donor cells (Figure 5E). This result establishes an in vivo, cell-intrinsic role for NKG2A on antigen-specific CD8$^+$ T cells in response to ECTV.

NKG2A Deficiency Does Not Affect Virus-Specific CD8$^+$ T Cells in a Cell-Extrinsic Manner

Although *Klrc1*$^{-/-}$ CD8$^+$ T cells are intrinsically less stable than their WT counterparts after ECTV infection, it remained possible that T-cell-extrinsic mechanisms, such as NK-cell-mediated killing of DCs or T cells, might also contribute to the dysfunctional CD8$^+$ T cell response in *Klrc1*$^{-/-}$ mice. To determine whether any other NKG2A-expressing cell affects the CD8$^+$ T cell response in vivo, we designed another adoptive transfer experiment that would allow us to observe how donor WT B8R-specific CD8$^+$ T cells survived in either a WT or *Klrc1*$^{-/-}$ host environment after ECTV infection (Figure 5F). CD45.1 WT B8R-specific CD8$^+$ T cells survived equally well in both WT and *Klrc1*$^{-/-}$ CD45.2 hosts, as judged by the number of B8R-H2-K^{b+}CD45.1$^+$ donor cells present in host spleens 7 dpi with WT-ECTV (Figure 5G). Finally, several reports have indicated that NK cells are capable of killing virus-specific T cells or otherwise impeding their priming (Andrews et al., 2010; Crouse et al., 2014; Lu et al., 2007; Schuster et al., 2014; Waggoner et al., 2010, 2012; Xu et al., 2014). We therefore depleted NK cells prior to ECTV infection to assess whether CD8$^+$ T cell numbers could be restored in the absence of NK cells. However, we found that antigen-specific CD8$^+$ T cells were highly reduced in both WT and *Klrc1*$^{-/-}$ spleens after NK cell depletion, indicating that NK cells probably function to control ECTV early enough to allow for the priming of an adequate CD8$^+$ T cell response (Figure 5H). Combined, this indicates that NKG2A expression on any cell other than the B8R-specific CD8$^+$ T cells appears to be unimportant for a functional specific T cell response.

Klrc1$^{-/-}$ ECTV-Specific CD8$^+$ T Cells Are More Susceptible to Apoptosis

To test whether the excessive apoptosis of ECTV-specific *Klrc1*$^{-/-}$-specific CD8$^+$ T cells was attributable directly to overactivation, we restimulated splenocytes from ECTV-infected mice ex vivo with increasing concentrations of plate-bound anti-CD3 antibody. After 2 days in culture with the plate-bound anti-CD3, we could not detect staining with the B8R-H2-K^b tetramer, suggesting that the CD8$^+$ T cell population was highly activated to the point of TCR downregulation (data not shown). Total CD8$^+$ T cells of *Klrc1*$^{-/-}$ mice exhibited consistently higher Annexin V and 7AAD staining compared to WT controls and overall were more sensitive to apoptosis after CD3-induced activation (Figure 5I). In contrast, CD4$^+$ T cells from both strains were equally sensitive to CD3-induced apoptosis, indicating that enhanced susceptibility was limited to *Klrc1*$^{-/-}$ CD8$^+$ T cells (Figure 5J). To determine whether *Klrc1*$^{-/-}$ ECTV-specific CD8$^+$ T cells were as susceptible to apoptosis as the total *Klrc1*$^{-/-}$ CD8$^+$ T cell population, CD8$^+$ T cell viability and apoptosis was determined after ex vivo stimulation with low amounts of IL-2, which would not downregulate TCR expression. Antigen-specific CD8$^+$ T cell numbers and Annexin V binding were measured 1, 3, and 5 days after culture with IL-2. WT cell numbers increased ex vivo, whereas *Klrc1*$^{-/-}$ cell numbers decreased over the same time period (Figure 5K, left). The inverse was true of Annexin V staining; fewer than 5% of WT cells were Annexin V$^+$ by day 3, but approximately 25% of the remaining *Klrc1*$^{-/-}$ cells were beginning to undergo apoptosis (Figure 5K, right). These data indicate that NKG2A can function specifically within activated CD8$^+$ T cells to modulate activation and prevent aberrant apoptosis.

Qa-1 Is Preferentially Expressed on B Cells in ECTV-Infected Tissues

Because NKG2A appears to function intrinsically within antigen-specific CD8$^+$ T cells, we reasoned that there must be an antigen-presenting cell (APC) population within an ECTV-infected secondary lymphoid tissue that expresses Qa-1 and can stimulate the CD8$^+$ T cell response. We found that naive splenic B cells expressed low, but detectable, amounts of Qa-1 and that B cells in ECTV-infected spleens upregulate Qa-1 expression (Figure 6A). In both naive and infected spleens, B cells expressed Qa-1 at higher amounts than non-B cells. Furthermore, when we infected WT and *Klrc1*$^{-/-}$ mice with the ova peptide-transgenic strain of ECTV used for the adoptive transfer immunizations, B cells in popliteal lymph nodes at 3 dpi were activated and presented the ova peptide, as detected by a SIINFEKL-H2-K^b-specific antibody. Thus, B cells are capable of both priming CD8$^+$ T cells and interacting with CD94/NKG2A heterodimers (Figure 6B). A similar observation was made in spleens at 7 dpi, with both WT and *Klrc1*$^{-/-}$ B cells presenting ECTV-derived

(K) WT and *Klrc1*$^{-/-}$ splenocytes were isolated 7 days after ECTV infection and cultured in complete RPMI containing 13 ng/ml rhIL-2. At 1, 3, and 5 days after culture, numbers of CD8$^+$B8R-H2-K^{b+} cells were quantified (left) and assessed for Annexin V staining (right).

All panels depict WT cells (filled circles/bars) and *Klrc1*$^{-/-}$ cells (open circles/bars). All data are representative of at least two independent experiments and were analyzed by multiple t tests. Mean ± SEM is represented on relevant graphs.

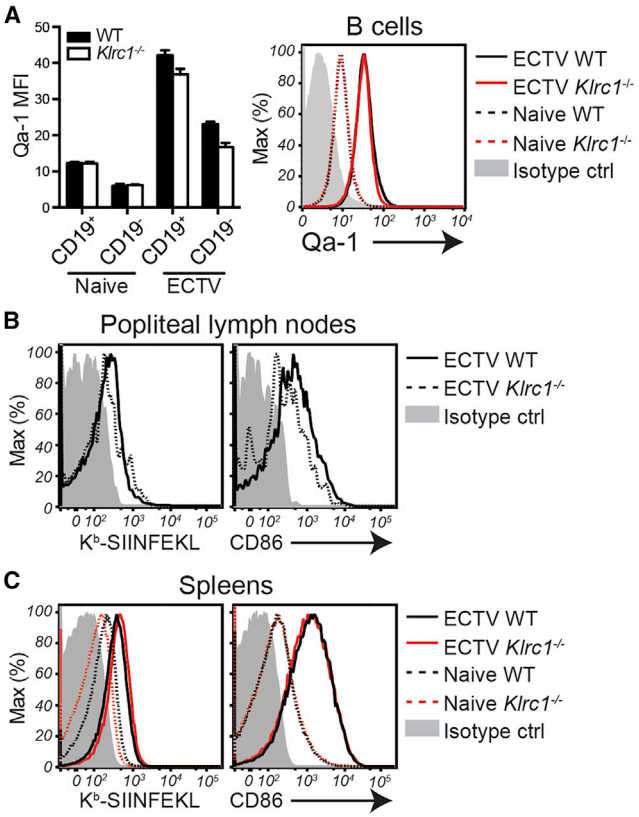

Figure 6. Qa-1 Is Preferentially Expressed on ECTV-Activated B Cells

(A) Splenocytes from naive or ECTV-infected mice were assessed for Qa-1 expression. Qa-1 MFI of $CD19^+$ versus $CD19^-$ splenocytes is shown on the left. Expression of Qa-1 on splenic B cells from naive or ECTV-infected mice is shown on the right.

(B) $CD19^+$ popliteal lymph nodes B cells were assessed for H2-K^b-SIINFEKL and CD86 expression with specific antibodies 3 days after infection with EV/NP-S-GFP.

(C) $CD19^+$ splenic B cells were assessed H2-K^b-SIINFEKL and CD86 expression 7 days after infection with EV/NP-S-GFP or from uninfected naive B cells.

Data are representative of at least three independent experiments. Mean ± SEM is represented on relevant graphs. Further supporting evidence can be found in Figure S4.

antigen and undergoing activation (Figure 6C). Given the relative dominance of B cell numbers in the nodes and spleen, we hypothesize that B cells are the dominant APCs responsible for activating $CD8^+$ T cells and interacting with CD94/NKG2A heterodimers after ECTV infection.

NKG2A Is Dispensable for Control of LCMV, VSV, and VV Infections

ECTV is somewhat unusual among mouse models of viral infection in that it is a natural pathogen that is acutely lethal in many murine strains at low infectious doses and hence requires robust innate and adaptive responses, even for subcutaneous infections of as little as 1,000 PFU of virus. We were therefore interested in determining whether NKG2A is broadly necessary for combating viral infections and, furthermore, how different viruses would affect the $CD8^+$ T cell response in the absence of NKG2A. To do this, we chose to infect WT and *Klrc1*$^{-/-}$ mice with nonlethal viruses that cause either acute (VSV-ova) or chronic (LCMV clone 13) infection in C57BL/6 mice, as well as with VV, an attenuated orthopoxvirus that is highly homologous to ECTV. VSV-ova splenic viral loads were similar in *Klrc1*$^{-/-}$ and WT mice 8 hr after infection (Figure S4A). At 7 dpi, after replicating virus was cleared from C57BL/6 mice, the specific $CD8^+$ T cell response in *Klrc1*$^{-/-}$ spleens was similar to WT controls, as judged by ova-H2-K^b-tetramer staining (Figure S4B). At 15 dpi with LCMV clone 13, viral loads in spleen, liver, kidney, and lung were all equivalent in *Klrc1*$^{-/-}$ and WT C57BL/6 mice (Figure S4C). After infection with VV, WT and *Klrc1*$^{-/-}$ mice lost little or no weight (Figure S4D) and had equivalent frequencies of specific and total $CD8^+$ T cells in spleens and draining lymph nodes (Figures S4E and S4F). Together, these data indicate that NKG2A might be necessary in antigen-activated T cells only during acute infections by highly replicative and cytopathic viruses, or perhaps specifically during ECTV infection.

DISCUSSION

In this study we have shown that *Klrc1*$^{-/-}$ mice are highly susceptible to infection by the mouse natural pathogen ECTV due to a defect in virus-specific $CD8^+$ T cell responses. This defect is cell intrinsic, as NKG2A expression is required to prevent excessive activation and AICD of virus-specific $CD8^+$ T cells. It is noteworthy that NKG2A is essential for host survival after ECTV infection but is not required for responses to an attenuated poxvirus, VV, or other viruses tested in our study, including VSV and LCMV. This result suggests that evolution of the *Klrc* locus might have been driven by pressure imposed by deadly poxvirus infections that cause excessive stimulation of $CD8^+$ T cells.

One previous study found that CD94-deficient (*Klrd1*$^{-/-}$) mice are also highly susceptible to ECTV infection (Fang et al., 2011). However, susceptibility was associated with defective expression and function of NKG2E on NK cells. Our analysis of WT and *Klrc1*$^{-/-}$ mice revealed essentially no expression of NKG2C or NKG2E on NK cells, which is consistent with several other studies (Kawamura et al., 2009; Vance et al., 1999, 2002). Moreover, if undetected CD94/NKG2E heterodimers could mediate ECTV clearance, we would expect *Klrc1*$^{-/-}$ mice to be more resistant to ECTV infection than WT mice, because CD94/NKG2E-mediated activation would not be countered by NKG2A-mediated inhibition. Thus, susceptibility of *Klrd1*$^{-/-}$ mice to ECTV seems most likely due to lack of CD94/NKG2A heterodimers rather than lack of CD94/NKG2E heterodimers. However, because *Klrd1*$^{-/-}$ mice were generated on the 129 background and backcrossed onto C57BL/6 mice (Fang et al., 2011), it is also possible that the *Klrc* locus remained 129 in these mice and that the activating isoforms of NKG2X are expressed and functional in this background. Whatever the case, both studies highlight the importance of the *Klrc* locus in the control of acute poxvirus infections.

It is clear from our data that impaired $CD8^+$ T cell responses in ECTV-infected *Klrc1*$^{-/-}$ mice are due to a T-cell-intrinsic rather than a T-cell-extrinsic defect. Why does lack of NKG2A have a dramatic effect during acute ECTV infection but no impact on VV, LCMV, and VSV infections? NKG2A-mediated inhibition

might be essential during anti-ECTV responses because ECTV is a natural pathogen that is highly replicative and might provoke extreme antigenic stimulation of $CD8^+$ T cells. ECTV is also highly cytopathic and aggressively infects secondary lymphoid tissues, such as the spleen and popliteal lymph nodes, disrupting their architecture (Esteban and Buller, 2005). This could attenuate initial T cell priming and further stress the relatively few virus-specific T cells that need to control infection in a highly inflammatory environment. In this scenario, the lack of NKG2A, which restrains overactivation, might have catastrophic effects.

It is also possible that during non-ECTV infections other inhibitory receptor-ligand interactions contribute more than NKG2A to finely tune $CD8^+$ T cell activation. This has been demonstrated during chronic LCMV infection, in which the absence of the inhibitory receptor 2B4 results in a suboptimal T cell response and exacerbated chronic disease (Waggoner et al., 2010). Although it was recently shown that T cells express Qa-1 during chronic LCMV infection, perhaps protecting them from NK-cell-mediated lysis by engaging CD94/NKG2A heterodimers (Xu et al., 2014), in our study, lack of NKG2A did not impact the course of chronic LCMV infection. NKG2A was also dispensable for sustaining specific $CD8^+$ T cells during influenza virus and adenovirus infections, but did limit immunopathology (Ely et al., 2014). Thus, we postulate that NKG2A might have various effects during different viral infections. These effects include preventing extreme activation and AICD (ECTV infection); limiting effector responses and immunopathology (influenza and adenovirus); no detectable impact due to the contribution of other inhibitory interactions (LCMV); and perhaps exhaustion and reduced control of viral replication (chronic infections yet to be identified).

During ECTV infection, all cells expressing Qa-1 can deliver an inhibitory signal to $NKG2A^+CD8^+$ T cells that prevents AICD. However, we noticed that B cells express Qa-1 at higher amounts than non-B cells in both naive and infected spleens. Furthermore, we demonstrated that B cells are infected by ECTV and present viral peptides, which has been corroborated by a recent study (Sei et al., 2015). Thus, B cells might be the dominant APCs that activate $CD8^+$ T cells and interact with CD94/NKG2A heterodimers during ECTV infection. Upon engagement, CD94/NKG2A heterodimers most likely optimize $CD8^+$ T cell activation through recruitment of SHP-1 and inhibition of tyrosine kinases, thereby preventing AICD. A similar mechanism was previously proposed for the ability of the human inhibitory receptor KIR2DL3 to attenuate AICD of memory $CD8^+$ T cells in response to peptide stimulation in vitro (Ugolini et al., 2001). Additionally, since the TCR co-receptor CD8 can bind to Qa-1, CD94/NKG2A heterodimers might be crucial for outcompeting CD8 binding and limiting CD8-mediated costimulation after initial T cell priming.

This study reshapes our understanding of surface expression of the *Klrc* locus-encoded receptors in mice. We demonstrate that mouse NKG2C and NKG2E are not expressed on the cell surface, at least in the B6 background. CD94 is mainly associated with NKG2A in $CD94^{hi}$ NK cells and $CD94^{hi}$ activated $CD8^+$ T cells. However, CD94 remains expressed on $CD94^{lo}$ NK cells in the absence of NKG2X as part of a complex with DAP12. Activated $CD8^+$ T cells express DAP10 but not DAP12, so it is likely CD94 pairs with DAP10 in activated $CD8^+$ T cells that lack NKG2X, although this conclusion should be conclusively confirmed through the generation of $Klrc1^{-/-} \times Hcst^{-/-}$ mice. These results are in agreement with a previous demonstration that mouse CD94 directly associates with DAP12 and DAP10 through a salt bridge in the transmembrane region without requiring NKG2C or NKG2E (Saether et al., 2011). Further studies will be essential to define the function of CD94/DAP12 and CD94/DAP10 complexes.

EXPERIMENTAL PROCEDURES

Mice

Klrc1$^{-/-}$ (Figure S1), WT C57BL/6J, *Hcst*$^{-/-}$, and B6.*Rag1*$^{-/-}$ mice were housed in specific-pathogen-free conditions at Washington University in St. Louis and St. Louis University. B6.SJL-Ptprca Pepcb/BoyJ mice ($CD45.1^+$ C57BL/6 strain) were purchased from Jackson Laboratory and subsequently bred in-house. *Tyrobp*$^{-/-}$ mice were generated by Toshiyuki Takai (Tohoku University). All animal studies were approved by the animal studies committees at Washington University School of Medicine in St. Louis and St. Louis University. Experiments were performed according to the animal care guidelines of the two institutions.

Viruses and Viral Infections

Plaque-purified ECTV (Moscow strain) was propagated on BS-C-1 cells. EV/NP-S-GFP contains a FluNP-SIINFEKL-GFP cassette in the disrupted V region (CrmC) of ECTV-Moscow (Parker et al., 2007). All ECTV and EV/NP-S-GFP infections were done in the foot pad (f.p.). at the indicated doses. ECTV viremia was assessed by quantitative real-time PCR of the EV107 gene. 5×10^6 PFU Indiana strain VSV-ova was injected intravenously (i.v.). LCMV clone 13 was administered i.v. at 2×10^6 PFU per mouse. Mice were infected in the f.p. with 1.25×10^7 PFU vaccinia SIINFEKL GFP virus (virus was provided by Dr. John Yewdell, NIAID). Viral loads were assessed from various tissues by standard plaque assays on BS-C-1 (for ECTV) or Vero (for VSV-ova, LCMV clone 13) cell monolayers.

Flow Cytometry

Antibodies, reagents, and staining methods can be found in the Supplemental Experimental Procedures. All samples were run on either a BD FACS Calibur or BD FACS Canto II system and analyzed with FlowJo software (Tree Star).

T Cell Restimulation Assay

Splenocytes from ECTV-infected mice were incubated overnight at 37°C in complete RPMI with either irrelevant peptide (SIINFEKL) or the poxvirus immunodominant peptide B8R (TSYKFESV). Supernatants were collected and IFN-γ concentration was measured with the Mouse Inflammation CBA kit (BD Biosciences). GM-CSF concentration was measured with Mouse GM-CSF ELISA Ready-SET-Go! (eBioscience). For intracellular detection of cytokines, cells were incubated for 6 hr in the presence of peptide and both brefeldin A (BD Biosciences) and monensin (eBioscience), then stained as described in the Supplemental Experimental Procedures.

RNA Isolation, Microarray, and Real-Time PCR Analysis

Cells were directly sorted into Buffer RLT Plus and RNA was isolated with the RNeasy Plus Micro kit (QIAGEN). All RNA samples were then processed and hybridized to Mouse Gene 1.0 ST arrays (Affymetrix) by Washington University's Genome Technology Access Center. Detailed information on microarray procedures and analysis can be found in the Supplemental Experimental Procedures. cDNA was synthesized with a SuperScript first-strand synthesis system (Invitrogen). Real-time quantitative PCR reactions were setup with iQ SYBR Green Supermix (Bio-Rad) and specific primers (see Supplemental Experimental Procedures) and run on a Bio-Rad iCycler.

T Cell Apoptosis Assay

Splenocytes from ECTV-infected mice were put into 96-well plates (2×10^6 cells/well) with complete RPMI supplemented with 13 ng/ml recombinant human IL-2 (Peprotech). 1, 3, and 5 days later, cells were stained with Annexin V and 7-AAD (PE Annexin V Apoptosis Detection Kit, BD PharMingen). B8R-$H2\text{-}K^b$-APC tetramers and anti-CD8-FITC antibody were added to the staining

cocktail to mark specific $CD8^+$ T cells. Cells were then analyzed by flow cytometry. In some experiments, splenocytes from ECTV-infected mice were cultured on plates coated with or without purified anti-CD3ε. After 2 days, cells were analyzed for the same apoptosis markers on either total $CD8^+$ or $CD4^+$ T cells.

Statistics

A Student's t test or multiple t tests were performed in Prism (GraphPad) in all cases. Mean ± SEM is represented on relevant graphs. *$p < 0.05$; **$p < 0.01$; ***$p < 0.001$; ****$p < 0.0001$.

ACCESSION NUMBERS

The accession number for the microarray data reported in this paper is GSE: GSE74780.

SUPPLEMENTAL INFORMATION

Supplemental Information includes four figures, one table, and Supplemental Experimental Procedures and can be found with this article online at http://dx.doi.org/10.1016/j.immuni.2015.11.005.

ACKNOWLEDGMENTS

M. Colonna was supported by the NIH grant 1R56AI119083-01, A.S.R. by the NIH training grant T32-AI007172, B.F.P. by the Rheumatic Diseases Core Center grant from the National Institute of Arthritis and Musculoskeletal and Skin Diseases (P30-AR048335), and W.M.Y. by the Howard Hughes Medical Institute. The authors thank the NIH Tetramer Core Facility (contract HHSN272201300006C) for provision of MHC tetramers, Scott Parker for technical assistance, John Yewdell for vaccinia virus, and Christina Song for help with preparing this manuscript.

Received: July 29, 2014
Revised: August 31, 2015
Accepted: November 5, 2015
Published: December 8, 2015

REFERENCES

Aldrich, C.J., DeCloux, A., Woods, A.S., Cotter, R.J., Soloski, M.J., and Forman, J. (1994). Identification of a Tap-dependent leader peptide recognized by alloreactive T cells specific for a class Ib antigen. Cell *79*, 649–658.

Andrews, D.M., Estcourt, M.J., Andoniou, C.E., Wikstrom, M.E., Khong, A., Voigt, V., Fleming, P., Tabarias, H., Hill, G.R., van der Most, R.G., et al. (2010). Innate immunity defines the capacity of antiviral T cells to limit persistent infection. J. Exp. Med. *207*, 1333–1343.

Biron, C.A. (2010). Expansion, maintenance, and memory in NK and T cells during viral infections: responding to pressures for defense and regulation. PLoS Pathog. *6*, e1000816.

Braud, V.M., Allan, D.S., O'Callaghan, C.A., Söderström, K., D'Andrea, A., Ogg, G.S., Lazetic, S., Young, N.T., Bell, J.I., Phillips, J.H., et al. (1998). HLA-E binds to natural killer cell receptors CD94/NKG2A, B and C. Nature *391*, 795–799.

Brownstein, D.G., and Gras, L. (1995). Chromosome mapping of Rmp-4, a gonad-dependent gene encoding host resistance to mousepox. J. Virol. *69*, 6958–6964.

Call, M.E., Wucherpfennig, K.W., and Chou, J.J. (2010). The structural basis for intramembrane assembly of an activating immunoreceptor complex. Nat. Immunol. *11*, 1023–1029.

Crouse, J., Bedenikovic, G., Wiesel, M., Ibberson, M., Xenarios, I., Von Laer, D., Kalinke, U., Vivier, E., Jonjic, S., and Oxenius, A. (2014). Type I interferons protect T cells against NK cell attack mediated by the activating receptor NCR1. Immunity *40*, 961–973.

Ely, K.H., Matsuoka, M., DeBerge, M.P., Ruby, J.A., Liu, J., Schneider, M.J., Wang, Y., Hahn, Y.S., and Enelow, R.I. (2014). Tissue-protective effects of NKG2A in immune-mediated clearance of virus infection. PLoS ONE *9*, e108385.

Esteban, D.J., and Buller, R.M. (2005). Ectromelia virus: the causative agent of mousepox. J. Gen. Virol. *86*, 2645–2659.

Fang, M., Orr, M.T., Spee, P., Egebjerg, T., Lanier, L.L., and Sigal, L.J. (2011). CD94 is essential for NK cell-mediated resistance to a lethal viral disease. Immunity *34*, 579–589.

Frebel, H., Nindl, V., Schuepbach, R.A., Braunschweiler, T., Richter, K., Vogel, J., Wagner, C.A., Loffing-Cueni, D., Kurrer, M., Ludewig, B., and Oxenius, A. (2012). Programmed death 1 protects from fatal circulatory failure during systemic virus infection of mice. J. Exp. Med. *209*, 2485–2499.

Gunturi, A., Berg, R.E., and Forman, J. (2003). Preferential survival of CD8 T and NK cells expressing high levels of CD94. J. Immunol. *170*, 1737–1745.

Kabat, J., Borrego, F., Brooks, A., and Coligan, J.E. (2002). Role that each NKG2A immunoreceptor tyrosine-based inhibitory motif plays in mediating the human CD94/NKG2A inhibitory signal. J. Immunol. *169*, 1948–1958.

Kawamura, T., Takeda, K., Kaneda, H., Matsumoto, H., Hayakawa, Y., Raulet, D.H., Ikarashi, Y., Kronenberg, M., Yagita, H., Kinoshita, K., et al. (2009). NKG2A inhibits invariant NKT cell activation in hepatic injury. J. Immunol. *182*, 250–258.

Lanier, L.L. (2008). Evolutionary struggles between NK cells and viruses. Nat. Rev. Immunol. *8*, 259–268.

Le Dréan, E., Vély, F., Olcese, L., Cambiaggi, A., Guia, S., Krystal, G., Gervois, N., Moretta, A., Jotereau, F., and Vivier, E. (1998). Inhibition of antigen-induced T cell response and antibody-induced NK cell cytotoxicity by NKG2A: association of NKG2A with SHP-1 and SHP-2 protein-tyrosine phosphatases. Eur. J. Immunol. *28*, 264–276.

Lee, N., Llano, M., Carretero, M., Ishitani, A., Navarro, F., López-Botet, M., and Geraghty, D.E. (1998). HLA-E is a major ligand for the natural killer inhibitory receptor CD94/NKG2A. Proc. Natl. Acad. Sci. USA *95*, 5199–5204.

Lin, C.C., Bradstreet, T.R., Schwarzkopf, E.A., Sim, J., Carrero, J.A., Chou, C., Cook, L.E., Egawa, T., Taneja, R., Murphy, T.L., et al. (2014). Bhlhe40 controls cytokine production by T cells and is essential for pathogenicity in autoimmune neuroinflammation. Nat. Commun. *5*, 3551.

Lu, L., Ikizawa, K., Hu, D., Werneck, M.B., Wucherpfennig, K.W., and Cantor, H. (2007). Regulation of activated CD4+ T cells by NK cells via the Qa-1-NKG2A inhibitory pathway. Immunity *26*, 593–604.

McMahon, C.W., Zajac, A.J., Jamieson, A.M., Corral, L., Hammer, G.E., Ahmed, R., and Raulet, D.H. (2002). Viral and bacterial infections induce expression of multiple NK cell receptors in responding CD8(+) T cells. J. Immunol. *169*, 1444–1452.

Miller, J.D., Peters, M., Oran, A.E., Beresford, G.W., Harrington, L., Boss, J.M., and Altman, J.D. (2002). CD94/NKG2 expression does not inhibit cytotoxic function of lymphocytic choriomeningitis virus-specific CD8+ T cells. J. Immunol. *169*, 693–701.

Moser, J.M., Gibbs, J., Jensen, P.E., and Lukacher, A.E. (2002). CD94-NKG2A receptors regulate antiviral CD8(+) T cell responses. Nat. Immunol. *3*, 189–195.

Odorizzi, P.M., and Wherry, E.J. (2012). Inhibitory receptors on lymphocytes: insights from infections. J. Immunol. *188*, 2957–2965.

Parker, A.K., Parker, S., Yokoyama, W.M., Corbett, J.A., and Buller, R.M. (2007). Induction of natural killer cell responses by ectromelia virus controls infection. J. Virol. *81*, 4070–4079.

Rygiel, T.P., Rijkers, E.S., de Ruiter, T., Stolte, E.H., van der Valk, M., Rimmelzwaan, G.F., Boon, L., van Loon, A.M., Coenjaerts, F.E., Hoek, R.M., et al. (2009). Lack of CD200 enhances pathological T cell responses during influenza infection. J. Immunol. *183*, 1990–1996.

Saether, P.C., Hoelsbrekken, S.E., Fossum, S., and Dissen, E. (2011). Rat and mouse CD94 associate directly with the activating transmembrane adaptor proteins DAP12 and DAP10 and activate NK cell cytotoxicity. J. Immunol. *187*, 6365–6373.

Schuster, I.S., Wikstrom, M.E., Brizard, G., Coudert, J.D., Estcourt, M.J., Manzur, M., O'Reilly, L.A., Smyth, M.J., Trapani, J.A., Hill, G.R., et al. (2014). TRAIL+ NK cells control CD4+ T cell responses during chronic viral infection to limit autoimmunity. Immunity *41*, 646–656.

Sei, J.J., Haskett, S., Kaminsky, L.W., Lin, E., Truckenmiller, M.E., Bellone, C.J., Buller, R.M., and Norbury, C.C. (2015). Peptide-MHC-I from endogenous antigen outnumber those from exogenous antigen, irrespective of APC phenotype or activation. PLoS Pathog. *11*, e1004941.

Sullivan, L.C., Clements, C.S., Beddoe, T., Johnson, D., Hoare, H.L., Lin, J., Huyton, T., Hopkins, E.J., Reid, H.H., Wilce, M.C., et al. (2007). The heterodimeric assembly of the CD94-NKG2 receptor family and implications for human leukocyte antigen-E recognition. Immunity *27*, 900–911.

Taylor, L.S., Paul, S.P., and McVicar, D.W. (2000). Paired inhibitory and activating receptor signals. Rev. Immunogenet. *2*, 204–219.

Tomasec, P., Braud, V.M., Rickards, C., Powell, M.B., McSharry, B.P., Gadola, S., Cerundolo, V., Borysiewicz, L.K., McMichael, A.J., and Wilkinson, G.W. (2000). Surface expression of HLA-E, an inhibitor of natural killer cells, enhanced by human cytomegalovirus gpUL40. Science *287*, 1031.

Ugolini, S., Arpin, C., Anfossi, N., Walzer, T., Cambiaggi, A., Förster, R., Lipp, M., Toes, R.E., Melief, C.J., Marvel, J., and Vivier, E. (2001). Involvement of inhibitory NKRs in the survival of a subset of memory-phenotype CD8+ T cells. Nat. Immunol. *2*, 430–435.

Vance, R.E., Kraft, J.R., Altman, J.D., Jensen, P.E., and Raulet, D.H. (1998). Mouse CD94/NKG2A is a natural killer cell receptor for the nonclassical major histocompatibility complex (MHC) class I molecule Qa-1(b). J. Exp. Med. *188*, 1841–1848.

Vance, R.E., Jamieson, A.M., and Raulet, D.H. (1999). Recognition of the class Ib molecule Qa-1(b) by putative activating receptors CD94/NKG2C and CD94/NKG2E on mouse natural killer cells. J. Exp. Med. *190*, 1801–1812.

Vance, R.E., Jamieson, A.M., Cado, D., and Raulet, D.H. (2002). Implications of CD94 deficiency and monoallelic NKG2A expression for natural killer cell development and repertoire formation. Proc. Natl. Acad. Sci. USA *99*, 868–873.

Waggoner, S.N., Taniguchi, R.T., Mathew, P.A., Kumar, V., and Welsh, R.M. (2010). Absence of mouse 2B4 promotes NK cell-mediated killing of activated CD8+ T cells, leading to prolonged viral persistence and altered pathogenesis. J. Clin. Invest. *120*, 1925–1938.

Waggoner, S.N., Cornberg, M., Selin, L.K., and Welsh, R.M. (2012). Natural killer cells act as rheostats modulating antiviral T cells. Nature *481*, 394–398.

Xu, H.C., Grusdat, M., Pandyra, A.A., Polz, R., Huang, J., Sharma, P., Deenen, R., Köhrer, K., Rahbar, R., Diefenbach, A., et al. (2014). Type I interferon protects antiviral CD8+ T cells from NK cell cytotoxicity. Immunity *40*, 949–960.

Zeng, L., Sullivan, L.C., Vivian, J.P., Walpole, N.G., Harpur, C.M., Rossjohn, J., Clements, C.S., and Brooks, A.G. (2012). A structural basis for antigen presentation by the MHC class Ib molecule, Qa-1b. J. Immunol. *188*, 302–310.